Am J Physiol Gastrointest Liver Physiol 309: G443–G454, 2015.
First published July 16, 2015; doi:10.1152/ajpgi.00400.2014.

TAK1 is a key modulator of the profibrogenic phenotype of human ileal myofibroblasts in Crohn's disease

Alessia Rosaria Grillo,[1,2] Melania Scarpa,[3] Renata D'Incà,[2] Paola Brun,[1] Marco Scarpa,[3] Andrea Porzionato,[1] Raffaele De Caro,[1] Diego Martines,[2] Andrea Buda,[2] Imerio Angriman,[2] Giorgio Palù,[1] Giacomo Carlo Sturniolo,[2] and Ignazio Castagliuolo[1]

[1]*Department of Molecular Medicine, University of Padova, Padova, Italy;* [2]*Department of Surgery Oncology and Gastroenterology, University of Padova, Padova, Italy; and* [3]*Oncological Surgery Unit, Veneto Institute of Oncology IOV - IRCCS, Padova, Italy*

Submitted 10 November 2014; accepted in final form 6 July 2015

Grillo AR, Scarpa M, D'Incà R, Brun P, Scarpa M, Porzionato A, De Caro R, Martines D, Buda A, Angriman I, Palù G, Sturniolo GC, Castagliuolo I. TAK1 is a key modulator of the profibrogenic phenotype of human ileal myofibroblasts in Crohn's disease. *Am J Physiol Gastrointest Liver Physiol* 309: G443–G454, 2015. First published July 16, 2015; doi:10.1152/ajpgi.00400.2014.—Transforming growth factor (TGF)-β-activated kinase 1 (TAK1) signaling can mediate inflammatory responses as well as tissue remodeling. Intestinal mucosal myofibroblast (IMF) activation drives gut fibrosis in Crohn's disease (CD); however, the molecular pathways involved are largely unknown. Thus we investigated the yet-unknown expression and function of TAK1 in human CD-associated fibrosis. Ileal surgical specimens, ileal biopsies, and IMF isolated from controls and CD patients were analyzed for TAK1 and its active phosphorylated form (pTAK1) by Western blotting, immunohistochemistry, and real-time quantitative PCR. TAK1 pharmacological inhibition and silencing were used to assess its role in collagen and inflammatory cytokine synthesis in IMF. TAK1 and pTAK1 levels increased in ileum specimens from CD patients compared with controls and correlated to tissue fibrosis. Similarly, TAK1 mRNA in ileal biopsies of CD patients correlated with fibrogenic marker expression but not inflammatory cytokines. CD-derived IMF showed higher TAK1 and pTAK1 expression associated with increased collagen1(α)1 mRNA levels compared with control IMF. TGF-β1 promoted pTAK1 nuclear translocation and collagen synthesis. TAK1 inhibition or silencing significantly reduced TGF-β1-stimulated collagen production and normalized the profibrogenic phenotype of CD-derived IMF. Taken together, these data suggest that TAK1 activation and nuclear translocation induce and maintain a fibrogenic phenotype in the IMF. Thus the TAK1 signaling pathway may represent a suitable target to design new, antifibrotic therapies.

intestinal myofibroblasts; fibrogenesis; TAK1

CHRONIC INFLAMMATION INVOLVING any gut segment whose main feature is tissue scarring and transmural fibrosis characterizes Crohn's disease (CD), in contrast to ulcerative colitis (UC), which involves the colon and infrequently causes massive intestinal fibrosis (42). Although fibrosis is considered the CD stigmata and can affect any intestinal segment involved, only CD patients that present ileal disease will develop symptoms due to intestinal stenosis within 10 yr from the diagnosis (8). Following surgical resection, this cluster of patients will have a high likelihood to experience a recurrence within 1 yr, supporting the existence of subgroups of CD patients with different phenotypes and clinical history (43). Although many studies have shed light on the involvement of different cellular populations and the molecular mechanism(s) responsible for the massive intestinal fibrosis in CD patients, our understanding of this process is, by far, unsatisfactory (42).

Fibrosis is considered the pathologic evolution of a healing process that occurs in tissues after a prolonged injury or a persistent inflammation (56). The persistence of a repair process leads to aberrant extracellular matrix (ECM) deposition, which in CD patients, causes increased thickness of the intestinal wall, loss of elasticity, and eventually, frank stenosis (41). Myofibroblasts are a key cellular population responsible for ECM homeostasis (56). Indeed, a tightly controlled balance between the production of ECM proteins and ECM-regulatory proteins by activated myofibroblasts is required to ensure proper ECM turnover (18, 39). These cells mainly derive from tissue resident fibroblasts, recruited and stimulated by locally produced growth factors and cytokines (32). In the normal intestine, few myofibroblasts are present, identified as α-smooth muscle actin (α-SMA)-positive and desmin-negative cells, and they exist as a widespread syncytium, tightly opposed to epithelial cells mainly in the crypts (39). During chronic inflammatory processes, such as CD, the extracellular milieu, rich in proinflammatory cytokines and growth factors, induces myofibroblast expansion and activation, which in turn, contribute to massive ECM deposition (3).

As transforming growth factor (TGF)-β induces myofibroblasts to synthesize and contract ECM, this cytokine plays a central role in the fibrotic response (6). Its receptors are overexpressed in the intestine of CD patients (33), and high TGF-β1 levels in the intestinal mucosa are predictive of stenotic recurrence following surgical resection (46). Although the mothers against decapentaplegic homolog (SMAD) cascade is the best known TGF-β1 signaling pathway, in recent years, several kinases have been implicated in TGF-β1 intracellular signaling (10). Among them, TGF-β-activated kinase 1 (TAK1) is a peculiar kinase, originally identified as a member of TGF-β-activated MKK kinase (MAP3K), shared by several intracellular signaling pathways (57). Thus experimental studies have demonstrated that TAK1 is implicated in cellular responses to environmental stress signaling (49) and cytokines, such as IL-1β and TNF (35, 45). However, this kinase is also recruited during responses orchestrated by pathogen-associated molecular pattern (PAMP) receptors, engaged by bacterial-derived endotoxins (e.g., LPS) (21). Once TAK1 is activated, as a consequence of threonines 184 and 187 and serine 192 phosphorylation (27, 50), it turns on many intracellular signal-

Address for reprint requests and other correspondence: I. Castagliuolo, Dept. of Molecular Medicine, Via Gabelli 63, Univ. of Padova, 35121 Padova, Italy (e-mail: ignazio.castagliuolo@unipd.it).

ing cascades, including MKK4/7 JNK (5, 19), MKK3/6-p38 MAPK cascade (17), and NF-κB, hence regulating a number of proinflammatory responses (21). Indeed, recent studies have reported that TGF-β1-mediated collagen and fibronectin expression in heart, kidney, and dermal mesenchymal cells involves TAK1 activation (16, 25, 26, 30, 58), thus revealing a new role for this kinase.

Therefore, we have investigated whether TAK1 expression and activity are modified in CD patients and whether this kinase is involved in the development of the fibrogenic phenotype in intestinal mucosal myofibroblasts (IMF).

MATERIALS AND METHODS

Patients enrollment and tissues collection. Twenty-six consecutive patients with inflammatory bowel disease (IBD), undergoing pancolonoscopy (Table 1), were enrolled in the study, in accordance with the Helsinki Declaration principles. The study received Institutional Review Board approval (NRC Protocol Number 2813P AOP), and all of those participating signed informed consent forms. CD and UC diagnosis and extension were determined by endoscopic, radiologic, and histological evaluations. Patients with Crohn's Disease Activity Index scores <150 and Truelove-Witts score (for UC patients) less than five—therefore, classified as being in remission—were recruited (17 CD and nine UC). Biopsies were taken from macroscopically noninflamed ileal mucosa. Biopsies were also collected from the ileum of 14 healthy subjects undergoing surveillance colonoscopy. In addition, full-thickness ileal specimens were obtained during surgical resections from 15 CD patients and during colectomies performed for sporadic, right colon carcinoma (at least at 10 cm from the margin of the lesions, $n = 9$; Table 1). Biopsies or surgical specimens were immediately placed in vials containing DMEM to purify IMF, snap frozen in liquid nitrogen for protein and RNA extraction, or fixed in buffered formalin for histological examination.

Quantification of intestinal fibrosis and inflammation. To assess collagen deposition in intestinal mucosa, we adapted a previously described histomorphometric method (51). Briefly, paraffin sections of full-thickness mucosal samples were simultaneously stained with both hematoxylin and eosin or with Sirius Red (saturated picric acid in distilled water 0.1% wt/vol). All samples were examined with a DM4500B microscope (Leica Microsystems, Wetzlar, Germany) connected with a DFC320 digital camera and software (Leica Microsystems) for image acquisition in a blinded fashion by two independent operators (A. Porzionato and A. R. Grillo). For each section, six images were captured, and quantitative data of Sirius Red staining were obtained using a computerized image analysis system (ImageJ; U.S. National Institutes of Health, Bethesda, MD) and expressed as percentage of Sirius Red-stained tissue over total area of the section.

To assess severity of mucosal inflammation, we quantified CXCL8 and TNF-α level by ELISA in surgical specimens. Briefly, tissues were homogenized in PBS, supplemented with a protease inhibitor mixture (Roche, Indianapolis, IN), and then centrifuged (13,000 *g* at 4°C). The clear supernatants were used to quantify CXCL8 and TNF-α by using commercial kits.

Isolation and culture of human IMF. Primary cultures of human IMFs were established, as described previously (29). In brief, mucosa was obtained by microdissection of full-thickness tissues and cut into small pieces; epithelial cells were removed by 30 min incubation (×2 times) in 2 mmol/l EDTA (Sigma, St. Louis, MO) in HBSS without Ca^{2+} and Mg^{2+} (Gibco, Life Technologies, Grand Island, NY). Then, mucosal samples were seeded in six-well plates and cultured in complete DMEM [containing 10% heat-inactivated fetal calf serum

Table 1. *Patients enrolled in the study*

Patients Enrolled during Pancolonoscopy			
	Crohn's Disease, $n = 17$	Ulcerative Colitis, $n = 9$	Control, $n = 14$
Gender (F/M)	8/9	4/5	5/9
Age, yr (range)	49 (32–70)	42 (24–75)	55 (24–66)
Mean disease duration, yr (SD)	11.8 (7.7)	14.7 (6.9)	
Age at onset:			
<17 yr old, *n* (%)	0 (0)	1 (11)	
17–40 yr old, *n* (%)	14 (82)	4 (44.5)	
>40 yr old,*n* (%)	3 (18)	4 (44.5)	
Treatment:			
Mesalamine, *n* (%)	17 (100)	9 (100)	
Azathioprine, *n* (%)	6 (35)	3 (33)	
Antibiotics, *n* (%)	3 (18)	0 (0)	
Steroids, *n* (%)	2 (12)	1 (11)	
Biologics, *n* (%)	1 (6)	0 (0)	
Disease behavior:			
Nonstricturing–nonpenetrating, *n* (%)	7 (41)		
Stricturing, *n* (%)	6 (35)		
Penetrating, *n* (%)	5 (29)		
Disease location, *n* (%)			
	Ileal, 4 (23.5)	Ulcerative proctitis, 1 (11)	
	Colonic, 4 (23.5)	Left-sided UC, 2 (22)	
	Ileocolonic, 7 (41)	Extensive UC, 6 (67)	
	Upper GI$^+$ ileocolonic, 2 (12)		

Patients Subjected to Ileocolectomy		
	Crohn's Disease, $n = 15$	Control (Right Colon Carcinoma), $n = 9$
Gender (F/M)	6/9	3/6
Age, yr (range)	41 (26–54)	65 (48–82)
Mean disease duration, yr (SD)	11.7 (2.9)	

UC, ulcerative colitis; GI, gastrointestinal.

(FCS), 1% nonessential amino acids, 100 U/ml penicillin, 100 μg/ml streptomycin, 50 μg/ml gentamycin, and 1 μg/ml amphotericin (all from Gibco, Life Technologies)]. IMF reached confluence within 1–2 wk. Cells were characterized at passage 4 for α-SMA and vimentin expression. Cultures >95% α-SMA$^+$ and vimentin$^+$ between passages 4 and 6 were used in all experiments.

IMFs were seeded at the required density, and after 24 h, medium was replaced with fresh DMEM containing 1% FCS. After 24 h, IMFs were exposed to recombinant human (rh)TGF-β1 (5 ng/ml; PeproTech, Rocky Hill, NJ), LPS from *Salmonella enterica* (1 μg/ml; Sigma), and muramyl dipeptide (MDP; 5 μg/ml; Sigma) or incubated with 10 μg/ml anti-TGF-β1 neutralizing antibody (EMD Millipore, Billerica, MA). Cells were harvested for RNA or protein extraction, fixed for immunocytochemistry, or subjected to [^{3}H]proline assay. Supernatants were collected for ELISA. When indicated, IMFs were incubated for 30 min with 2 μM 5Z-7-oxozeaenol (a TAK1 inhibitor; AnalytiCon Discovery GmbH, Potsdam, Germany) or vehicle before rhTGF-β1 exposure. In preliminary assays, 5Z-7-oxozeaenol, up to 4 μM, did not exert significant cytotoxic effects, as determined by 3-(4,5-dimethylthiazol-2-yl)-2,5-diphenyltetrazolium bromide (MTT) assays (data not shown).

Adenoviral vector generation and silencing experiments. Specific small interfering short hairpin (sh)RNA targeting TAK1 was expressed in IMF by using the BLOCK-iT Adenoviral RNAi Expression System (Invitrogen, Carlsbad, CA), according to the manufacturer's protocol. Briefly, shRNAs targeting TAK1 or the gene encoding β-galactosidase (LacZ) as controls were cloned into the shuttle vector pENTR/U6; a LR recombination was then performed with the pAd/BLOCK-iT-DEST plasmid containing the adenoviral genome without E1 and E3 regions. The adenoviral constructs obtained were enzymatically digested with Pac I and transfected into packaging 293A cells. The sequences encoding shRNA for TAK1 and LacZ, designed using the BLOCK-iT RNAi Designer (http://rnaidesigner.invitrogen.com/rnaiexpress/index.jsp; Life Technologies), were the following: shTAK1, 5′CACCGCAAGTTCCTGCCACAAATGACGAATCATTTGTGGCAGGAACTTGC3′, and shLacZ, 5′CACCGCTACACAAATCAGCGATTTCGAAAAATCGCTGATTTGTGTAG3′.

Recombinant adenoviral particles were titrated by the 50% tissue culture infective dose assay, and IMFs were transduced with a multiplicity of infection of 1:100 in DMEM containing 2% FCS, 72 h before other treatments. IMF, transduced with an adenoviral vector expressing shRNA targeting TAK1 (pAdShTAK1) or targeting LacZ (pAdShLacZ), did not show significant differences in cellular viability, as determined by MTT assays (data not shown).

Quantification of collagen synthesis by [^{3}H]proline incorporation. Collagen synthesis by IMF was quantified by [^{3}H]proline incorporation. Briefly, 3×10^4 IMFs were seeded into 12-well plates, cultured for 48 h in complete DMEM, and placed for 24 h in DMEM containing 1% FCS. When requested, cells were pretreated with the TAK1 inhibitor for 30 min before exposure to TGF-β1 or transduced with proper recombinant adenoviral vector, 72 h before TGF-β1 treatment. Then, 1 μCi/ml [^{3}H]proline (Perkin Elmer, Waltham, MA) was added to each well, and after 36 h, proteins of the culture media were precipitated by centrifugation in 10% (vol/vol) TCA solution. Cell monolayers were washed twice with PBS and lysed in 0.3 ml 10% SDS. Radioactivity was quantified, combining isovolumes of cell lysates and precipitated proteins, mixed to 5 ml scintillation cocktail using a beta counter (Tri-Carb 2810TR; Perkin Elmer). Total radioactivity, expressed as counts/minute, was normalized to the respective protein content, determined by bicinchoninic acid (BCA) protein assay (Pierce, Life Technologies).

Cytokine release. IMFs (2×10^3) were seeded on 96-well plates and cultured in 100 μl complete DMEM for 24 h. Then, the medium was removed and replaced with DMEM containing 1% FCS for an additional 24 h. Cells were then treated with 5Z-7-oxozeaenol (10 mM) or vehicle and after an additional 30 min, exposed to rhTGF-β (5 ng/ml), LPS (1 μg/ml), or MDP (5 μg/ml). The culture media were collected after 24 h and diluted 1:2 in PBS, and CXCL8 and IL-6 were quantified by commercially available ELISA kits (ImmunoTools, Friesoythe, Germany).

Western blotting. IMFs were lysed in ice-cold radioimmunoprecipitation assay buffer, whereas tissue samples were homogenized using a Retsch MM300 (Qiagen, Germantown, MD). Cellular debris was removed by centrifugation (13,000 *g*, 10 min), the clear supernatant collected, and the protein concentration determined by the BCA protein assay (Pierce, Life Technologies). A total of 50 μg proteins was fractionated through a 10% SDS gel and transferred to a polyvinylidene difluoride membrane (Bio-Rad Laboratories, Hercules, CA). Following 1 h incubation with PBS, containing 5% BSA (Sigma), membranes were incubated at 4°C for 16 h with rabbit anti-human TAK1, rabbit anti-human TAK1 phosphorylated form (pTAK1; Cell Signaling Technology, Danvers, MA), mouse anti-human α-SMA, mouse anti-human β-actin, mouse anti-human β-tubulin (Sigma), or goat anti-lamin A/C (a kind gift of Dr. G. Alvisi, Department of

Table 2. *Primers, probes, and conditions used in quantitative RT-PCR*

Gene	Accession Number	Primers and Probe Sequences	Amplicon, bp	T_a, °C
α-sma	NM_001613	FW 5′GGGACGACATGGAAAAGATCTG3′ RV 5′CAGGGTGGGATGCTCTTCAG3′ Fam-GGGACGACATGGAAAAGATCTG-Tamra	77	63
Col1α1	NM_000088	FW 5′GTCGAGGGCCAAGACGAA3′ RV 5′CACGTCTCGGTCATGGTACCT3′ Fam-ACATCCCACCAATCACTTGCGTACAGA-Tamra	75	64
Tak1	NM_003298	FW 5′CAAAGCTAAGTGGAGAGCAAAAGA3′ RV 5′GATAACTGCCGAAGCTCTACAATAA3′ Fam-TGCTATTAAACAAATAGAAAGTGAATCTGAGAG GAAAGC-Tamra	92	57
Timp1	NM_003254	FW 5′CACCCACAGACGGCCTTCT3′ RV 5′CTTCTGGTGTCCCCACGAACT3′ Fam-CAATTCCGACCTCGTCATCAGGGC-Tamra	67	62
Gapdh	NM_002046	FW 5′TGAACGGGAAGCTCACTGG3′ RV 5′GGTCCACCACTGACACGTTG3′ Fam-ATGGCCTTCCGTGTCCCCACTG-Tamra	73	60
Tnf	NM_000594	FW 5′CCCAGGGACCTCTCTCTAATC3′ RV 5′ATGGGCTACAGGCTTGTCACT3′ Fam-TGGCCCAGGCAGTCAGATCATC-Tamra	84	60

T_a, annealing temperature; *α-sma*, α-smooth muscle actin; FW, forward; RV, reverse; Fam, 6-carboxyfluorescein; Tamra, tetramethylrhodamine; *Col1α1*, collagen1(α)1; *Tak1*, transforming growth factor-β-activated kinase 1; *Timp1*, tissue inhibitor of metalloproteinase-1.

Molecular Medicine, University of Padova, Padova, Italy). Following extensive washes, membranes were incubated with horseradish peroxidase-labeled secondary antibodies. Then, immunocomplexes were visualized with the enhanced chemiluminescence Western blotting system (Santa Cruz Biotechnology, Santa Cruz, CA). Bands were quantified by scanning densitometry using VersaDoc Quantity One software (Bio-Rad Laboratories) with β-actin as a loading control.

Nuclear protein extraction. IMFs were incubated with the indicated stimuli for the specified times and then washed twice with ice-cold PBS. The cells were scraped and incubated for 10 min at 4°C into buffer A (10 mmol/l HEPES, 0.1 mmol/l EDTA, 0.1 mmol/l EGTA, 10 mmol/l KCl, 1 mmol DTT, 0.5 mmol PMSF, 1 mmol $NaVO_4$, 10 mmol NaF). Then, 2% Nonidet P-40 was added for an additional 2 min. The nuclei were precipitated by centrifugation at 13,000 *g*, and the clear supernatant was collected as cytoplasmic extracts. Nuclei were incubated in buffer B (20 mmol/l HEPES, 0.4 mol/l NaCl, 1 mmol/l EDTA, 1 mmol EGTA, 1 mmol DTT, 0.5 mmol PMSF, 1 mmol $NaVO_4$, 10 mmol NaF) for 30 min at 4°C. After centrifugation at 13,000 *g* for 2 min, the supernatant, which contains the nuclear proteins, was collected. Protein concentration was measured by the BCA protein assay. Proteins were then subjected to Western blot analysis, as described above.

Total RNA extraction and real-time quantitative RT-PCR. The SV Total RNA Isolation System (Promega, Madison, WI) was used to extract total RNA from IMF and ileal samples, according to the manufacturer's protocol. Tissues were homogenized in lysis buffer using a Retsch MM300 (Qiagen) for 5 min at 30 Hz. Contaminating DNA was removed by DNase I treatment (Promega). Total RNA (3 μg) was reverse transcribed to cDNA using random primers and the MuLV Reverse Transcriptase (Applied Biosystems, Life Technologies). Real-time quantitative PCR was performed on an ABI PRISM 7700 Sequence Detection System (Perkin Elmer) using specific 6-carboxyfluorescein-labeled probes and primers, designed using the program Primer Express. All probes have been designed, spanning exon junctions, to exclude the amplification of contaminating genomic DNA. Primer and probe sequences, as well as amplification conditions, are reported in Table 2. For each sample, the amounts of the targets and endogenous reference (GAPDH) were extrapolated from a standard curve, prepared using serially diluted correspondent cDNAs subcloned into the pGEM-T vector (Promega).

Confocal immunofluorescence microscopy. Confocal immunofluorescence microscopy was used to assess TAK1, pTAK1, and α-SMA tissue distribution and subcellular localization. To perform tissue immunohistochemistry, 5 μm cryosections, obtained from full-thickness gut specimens, were fixed in buffered 4% paraformaldehyde (PFA) for 10 min. To perform immunocytochemistry, 5×10^4 IMFs were seeded on glass coverslips and cultured for 24 h in complete DMEM. When required, cells were exposed to rhTGF-β1, LPS, or MDP for the specified time, then washed in cold PBS, and fixed in buffered 4% PFA for 5 min. Sections or cells were then washed, blocked in Tris-buffered saline (TBS) solution containing 2% BSA (wt/vol) and 0.03% Triton X-100 (vol/vol) for 30 min at room temperature, and then incubated for 1 h in a moisture chamber with anti-TAK1, anti-pTAK1, or anti-α-SMA antibodies. Sections were

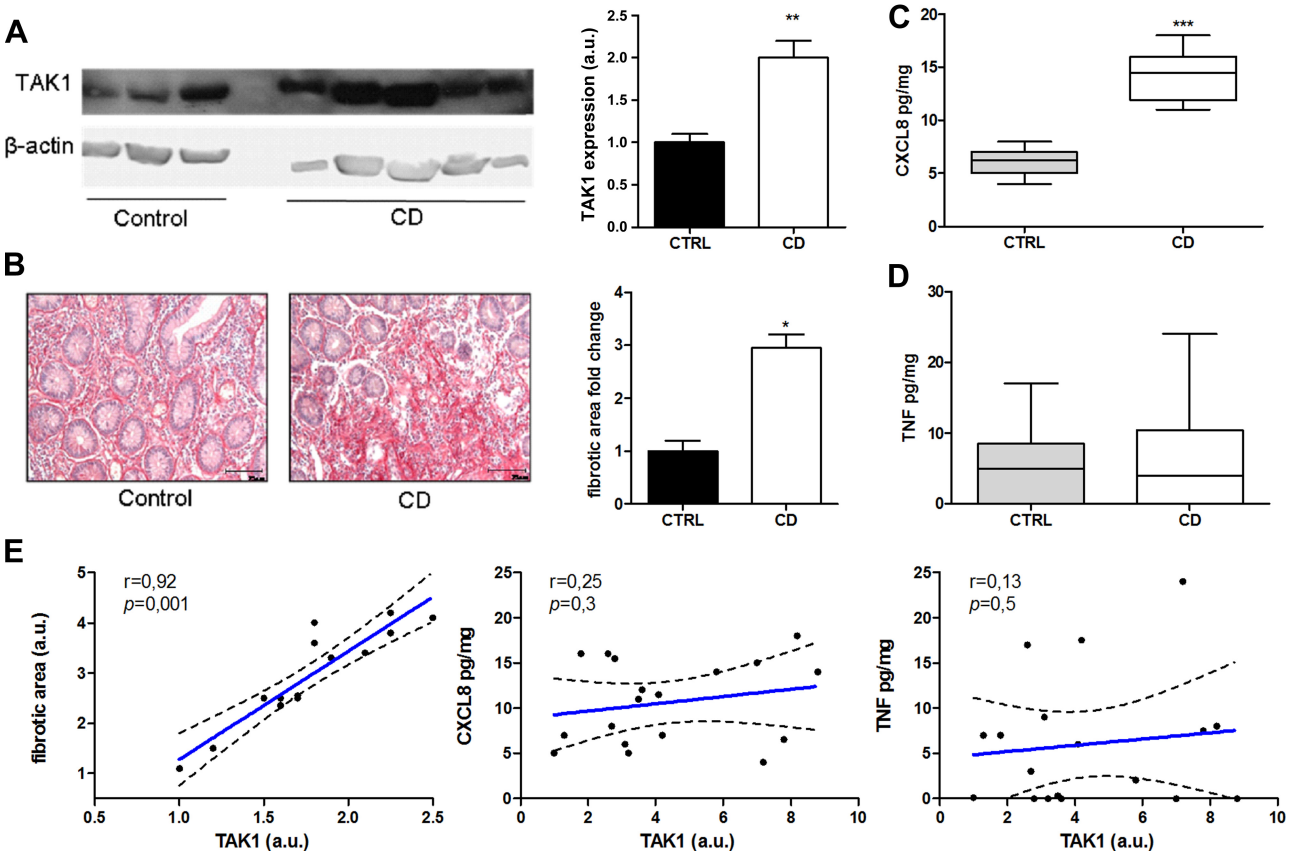

Fig. 1. Transforming growth factor (TGF)-β-activated kinase 1 (TAK1) is overexpressed in fibrotic tissue of Crohn's disease (CD) patients. *A*: Western blot analysis of TAK1 expression in ileal tissues obtained from normal ileum of patients ($n = 9$) with right colon carcinoma or stenotic segments of CD patients ($n = 15$) and relative densitometric analysis. *B*: Sirius Red staining of ileal sections obtained from normal ileum or stenotic segments of CD patients (scale bars, 75 μm) and relative Sirius Red staining quantification by ImageJ. Data are reported as means ± SE. $^{**}P < 0.01$ and $^{*}P < 0.05$ vs. control (CTRL). CXCL8 (*C*) and TNF (*D*) levels in ileal tissues measured by ELISA. Data are reported as box and whiskers of 2.5 and 97.5 percentiles of 8 determinations for control and 11 for CD. $^{***}P < 0.001$ vs. control. *E*: Pearson correlation analysis of TAK1 expression with ileal fibrotic areas, CXCL8, and TNF. Dashed lines show the 95% confidence band of the best fit line.

washed extensively in TBS and incubated with the appropriate FITC or tetramethylrhodamineisothiocyanate-labeled secondary antibody. To stain nuclei, cells were incubated for 10 min with TOTO-3 (Invitrogen). Specimens were washed, mounted, and observed using a TCS-NT/SP2 confocal microscope (Leica Microsystems) equipped with ×40 and ×63 objectives.

Statistical analysis. All data are shown as means ± SE. The Student's *t*-test was used for analysis of parametric data, whereas the Mann-Whitney *U*-test was used for evaluation of nonparametric data, and Pearson correlation test was applied for correlation analysis. $P < 0.05$ was considered statistically significant.

RESULTS

Increased TAK1 expression in ileum of CD patients. Initially, we asked whether TAK1 expression in the ileum correlates to the degree of fibrosis and/or inflammation in CD patients. To this end, we evaluated ileum specimens from CD patients who underwent surgery for intestinal stenosis and ileal biopsies from patients with CD in remission.

Surgical specimens obtained from CD patients with stenosis showed severe fibrosis, augmented inflammatory cytokine levels, and TAK1 expression compared with normal ileum taken from patients with colon adenocarcinoma (Fig. 1, *A–D*). Indeed, TAK1 expression directly correlated to the fibrotic area ($r = 0.92$), quantified by morphometric analysis of Sirius Red-stained sections (Fig. 1, *B* and *E*), but not to the inflammatory cytokine level (Fig. 1, *C–E*).

In ileal biopsies obtained from CD patients showing clinical and hematological parameters of disease remission, TNF-α mRNA levels were compared with ileal biopsies from healthy controls and UC patients (Fig. 2*C*), whereas collagen1(α)1 (COL1A1) and tissue inhibitor of metalloproteinase-1 (TIMP1) mRNA levels were increased significantly (Fig. 2, *A* and *B*). Strikingly, TAK1 mRNA expression, which was significantly higher in ileal biopsies of CD patients than in control and UC subjects (Fig. 2*D*), correlated directly with COL1A1 and TIMP1 mRNA levels but not with TNF-α mRNA (Fig. 2*E*),

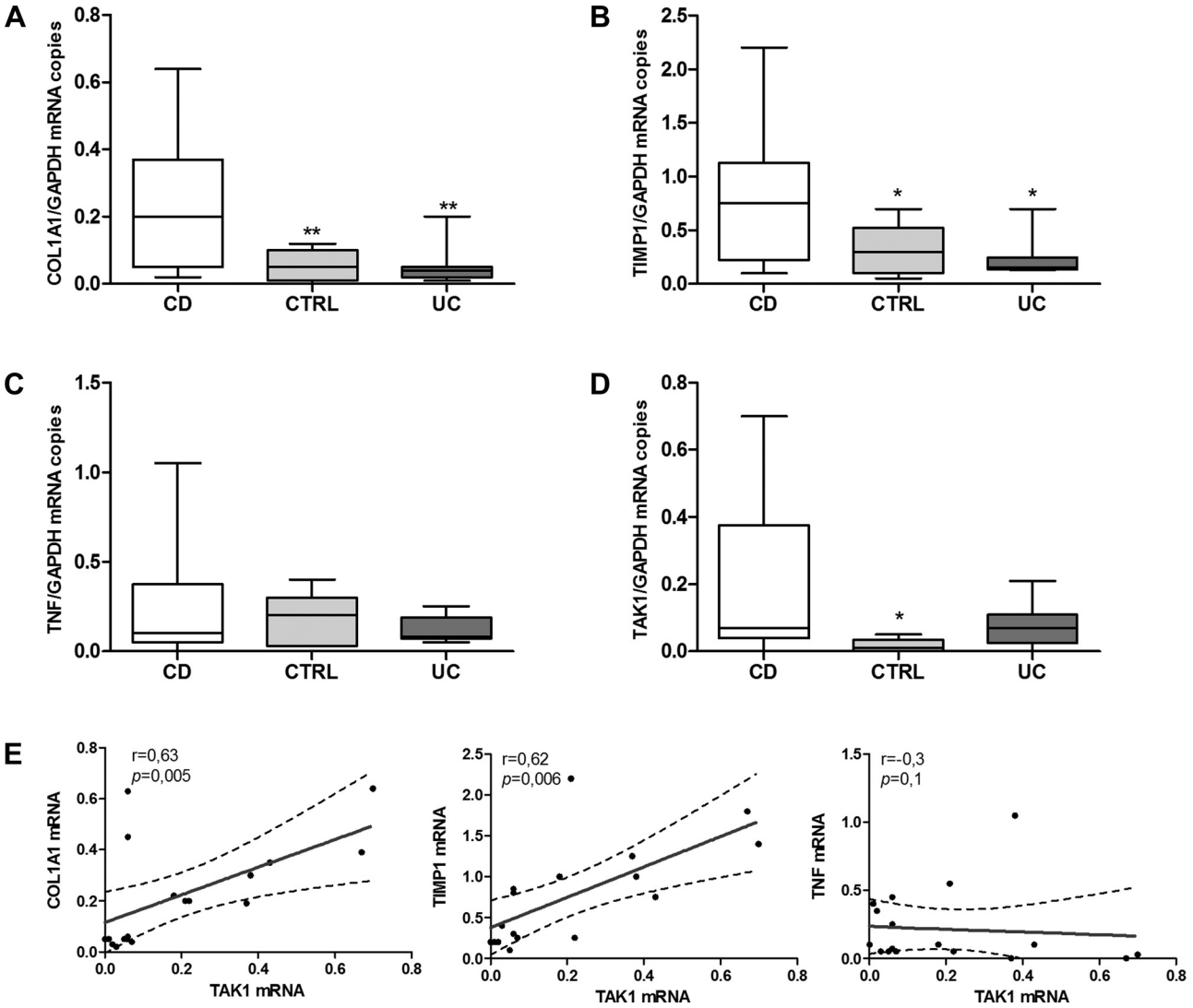

Fig. 2. TAK1 mRNA level correlates with fibrotic markers in the ileal mucosa of CD patients. *A–D*: collagen1(α)1 (COL1A1), tissue inhibitor of metalloproteinase-1 (TIMP1), TNF, and TAK1 mRNA levels, respectively, in biopsies of ileal mucosa of CD patients ($n = 17$), healthy control subjects ($n = 14$), and ulcerative colitis (UC) patients ($n = 9$). Data are reported as box and whiskers of 2.5 and 97.5 percentiles. *$P < 0.05$ and **$P < 0.01$ vs. CD. *E*: Pearson correlation analysis of TAK1 mRNA with COL1A1, TIMP1, and TNF mRNA of CD patients ($n = 17$). Dashed lines show the 95% confidence band of the best fit line.

supporting the view that TAK1 might be associated with fibrosis in CD patients.

IMFs are a source of TAK1 in CD patients. To identify the cellular source of TAK1, we performed immunohistochemistry on full-thickness ileal cryosections from CD and control subjects. TAK1 was expressed in the epithelial layer and in the periglandular area, where it colocalized with α-SMA-positive cells (Fig. 3*A*). In keeping with the known myofibroblasts hyperplasia in CD, a larger number of α-SMA$^+$ cells were detectable in the submucosal layer of CD patients compared with controls (Fig. 3, *A* and *B*). Notably, α-SMA levels correlated directly with TAK1 expression in the ileal mucosa of fibrostenosing CD ($r = 0.93$) by Pearson correlation analysis (Fig. 3*C*), suggesting that an expanded IMF cell population might contribute to the augmented levels of TAK1 in the ileal mucosa.

To substantiate the involvement of IMF in TAK1 overexpression in the intestinal mucosa, we established primary IMF cultures from ileal mucosa. In agreement with the strong TAK1 immunoreactivity detected (Fig. 3*D*), TAK1 mRNA and protein levels were significantly higher in CD-derived IMF than in cells isolated from normal ileum (Fig. 3, *E* and *F*). Taken together, these data suggest that the increased TAK1 levels in the ileal mucosa of CD patients are not merely due to the enhanced presence of IMF in the fibrotic intestine but also to its overexpression in IMF.

TAK1 is phosphorylated in fibrotic ileum and IMF of CD patients. We next established whether TAK1 overexpression was associated with an enhanced activation by using a specific antibody detecting TAK1 only when phosphorylated at both Thr184 and Thr187 residues. As shown in Fig. 4*A*, the ratio between TAK1 and pTAK1 in the fibrotic ileal mucosa of CD patients was 2.9-fold higher than in controls. Moreover, pTAK1 immunoreactivity drastically increased in ileal sections from CD patients and colocalized with subepithelial α-SMA$^+$ cells (Fig. 4*B*). Furthermore, the TAK1 activation state (pTAK1) was significantly more elevated in IMF derived from CD patients compared with control (2.6-fold increase; Fig. 4, *C* and *D*). Increased pTAK1 levels in CD-derived IMFs were largely due to autocrine TGF-β1 activity, since pTAK1 was completely abolished by the addition to the culture medium of a neutralizing anti-TGF-β1 antibody (Fig. 4*E*).

Profibrogenic stimuli induce pTAK1 nuclear translocation in IMF. Since previous studies have reported that TAK1 can mediate signal transduction pathways triggered by both profibrogenic and proinflammatory stimuli, we assessed their effect on TAK1 activation in IMF. In control IMF, pTAK1 was barely detectable and mainly localized to the cytoplasm (Fig. 5*A*). Stimulation with TGF-β1, LPS, or MDP could induce an increase of pTAK1 staining (Fig. 5*A*). However, only in TGF-β1-treated IMF could we observe a

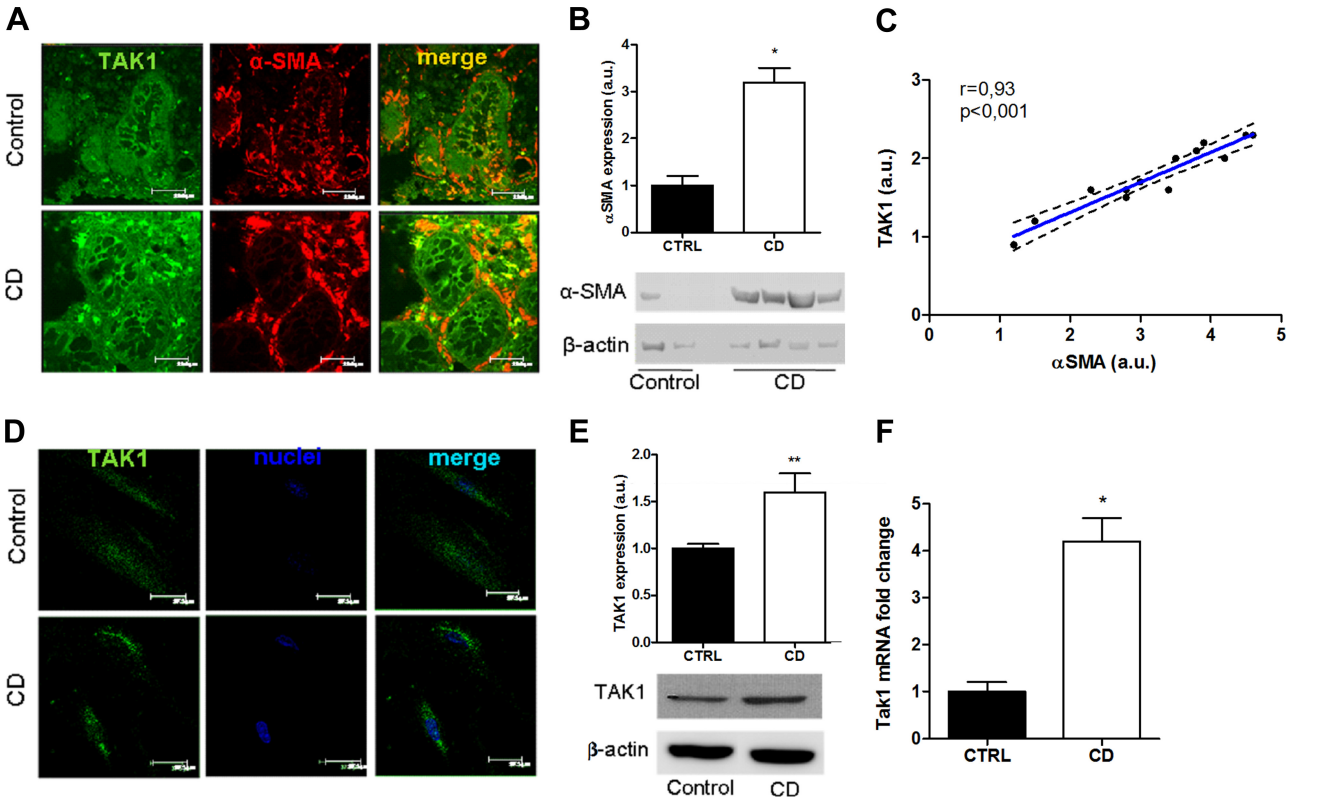

Fig. 3. TAK1 is overexpressed in CD-derived intestinal mucosal myofibroblast (IMF). *A*: tissue sections of ileum obtained from control patients with right colon carcinoma ($n = 9$) or stenotic segments of CD patients ($n = 15$) were stained for TAK1. α-Smooth muscle actin (α-SMA) was used as a myofibroblast marker (scale bars, 23.8 μm). *B*: Western blotting analysis of α-SMA on ileal tissues obtained from normal ileum ($n = 9$) or stenotic segments ($n = 15$) of CD patients and relative densitometric analysis. *C*: Pearson correlation analysis of Western blot data of α-SMA with TAK1 expression in stenotic segments. Dashed lines show the 95% confidence band of the best fit line. *D*: immunofluorescence analysis of TAK1 in IMF obtained from normal ileum controls ($n = 3$) and CD ($n = 3$; scale bars, 37.5 μm). *E*: Western blotting analysis of TAK1 on IMF obtained from normal ileum or stenotic segments of CD patients and densitometric analysis. *F*: real-time quantitative PCR (qPCR) for TAK1 in IMF obtained from normal ileum ($n = 4$) or stenotic segment of CD ($n = 4$) patients. Data are reported as means ± SE. $^{**}P < 0.05$ and $^{*}P < 0.01$ vs. control.

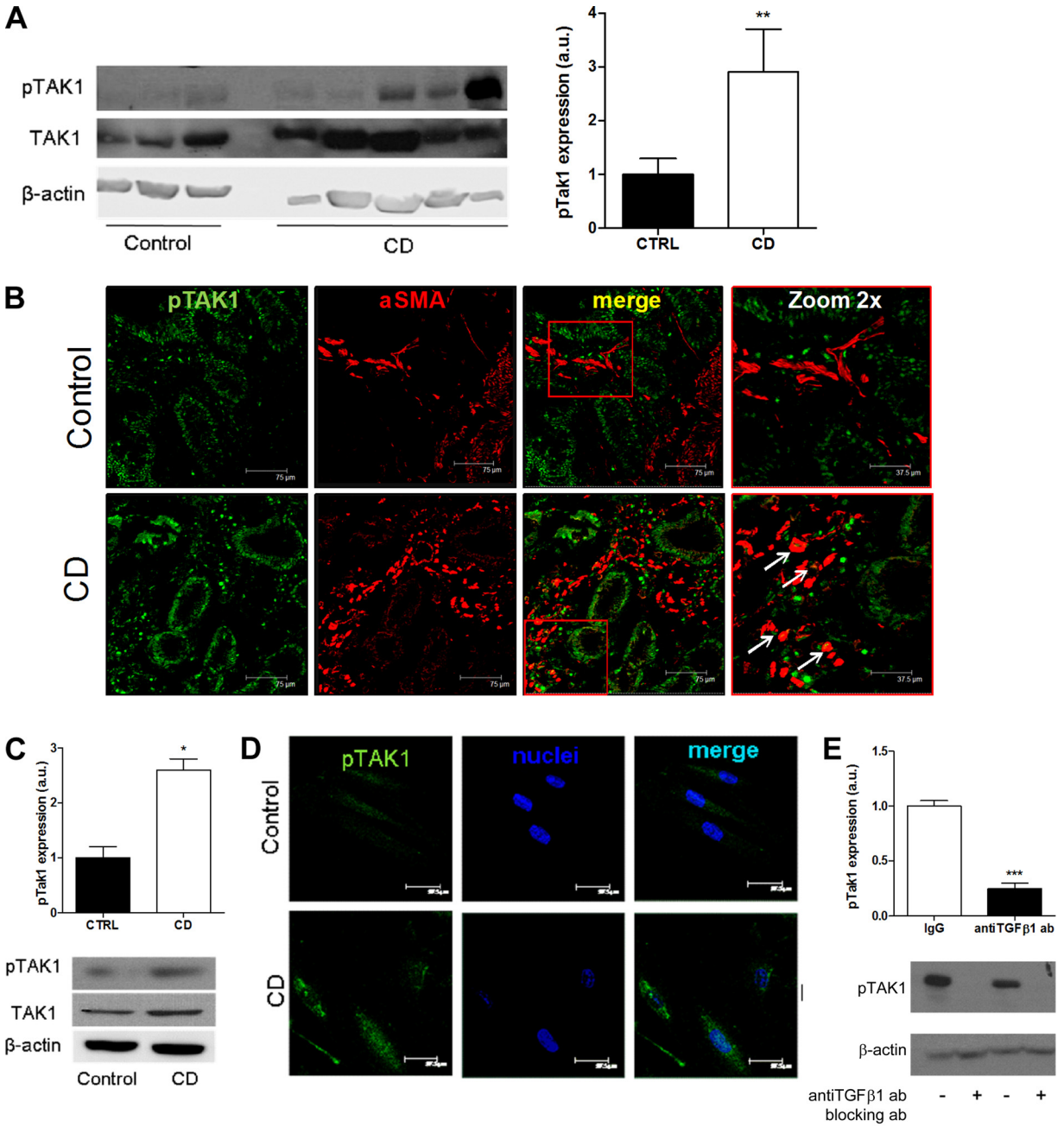

Fig. 4. TAK1 activation in IMF of CD patients. *A*: Western blotting analysis of phosphorylated (p)TAK1 in specimens obtained from normal ileum ($n = 9$) or stenotic segments of CD patients ($n = 15$) and relative densitometric analysis. *B*: tissue sections of ileum obtained from control patients with right colon carcinoma ($n = 9$) or stenotic segments of CD patients ($n = 15$) were stained for pTAK1. α-SMA was used as a myofibroblast marker (scale bars, 23.8 μm). Arrows, pTAK1$^+$ α-SMA$^+$ myofibroblasts. *C*: Western blotting of pTAK1 in IMF derived from control subjects and CD patients ($n = 4$–5 cell lines for each group) and relative densitometric analysis. *D*: immunocytochemical analysis of pTAK1 in control and CD-derived IMF (scale bars, 37.5 μm; $n = 3$ cell lines for each group). *E*: Western blotting analysis of pTAK1 on CD-derived IMF treated with 10 μg/ml anti-TGF-β neutralizing antibody (ab) for 3.5 h and relative densitometric analysis ($n = 4$). Data are reported as means ± SE. ***$P < 0.001$, **$P < 0.05$, and *$P < 0.01$ vs. control.

pronounced nuclear localization of pTAK1. To confirm the observed nuclear translocation of TAK1, nuclear and non-nuclear fractions were prepared from IMF treated with TGF-β1 for 30 min. The microtubule protein β-tubulin and the nuclear protein lamin A were used as markers to confirm the purity of the respective fractions. As shown in Fig. 5*C*, pTAK1 was expressed in both the nuclear and non-nuclear fractions and displayed the same accentuated response to stimulation with TGF-β1, described in both total cell lysate Western blots (Fig. 5*B*) and immunocytochemistry (Fig. 5*A*).

Next, we analyzed the specific contribution of TAK1 to IMF phenotype. In line with the well-known proinflammatory effect of bacterial endotoxins in IMF, LPS, as opposed to TGF-β1, induced CXCL8 and IL-6 secretion by IMF (Fig. 6, *A* and *B*). Moreover, LPS-induced inflammatory cytokine release was partially inhibited by a TAK1 inhibitor, 5Z-7-oxozeaenol (Fig. 6, *A* and *B*). On the other hand,

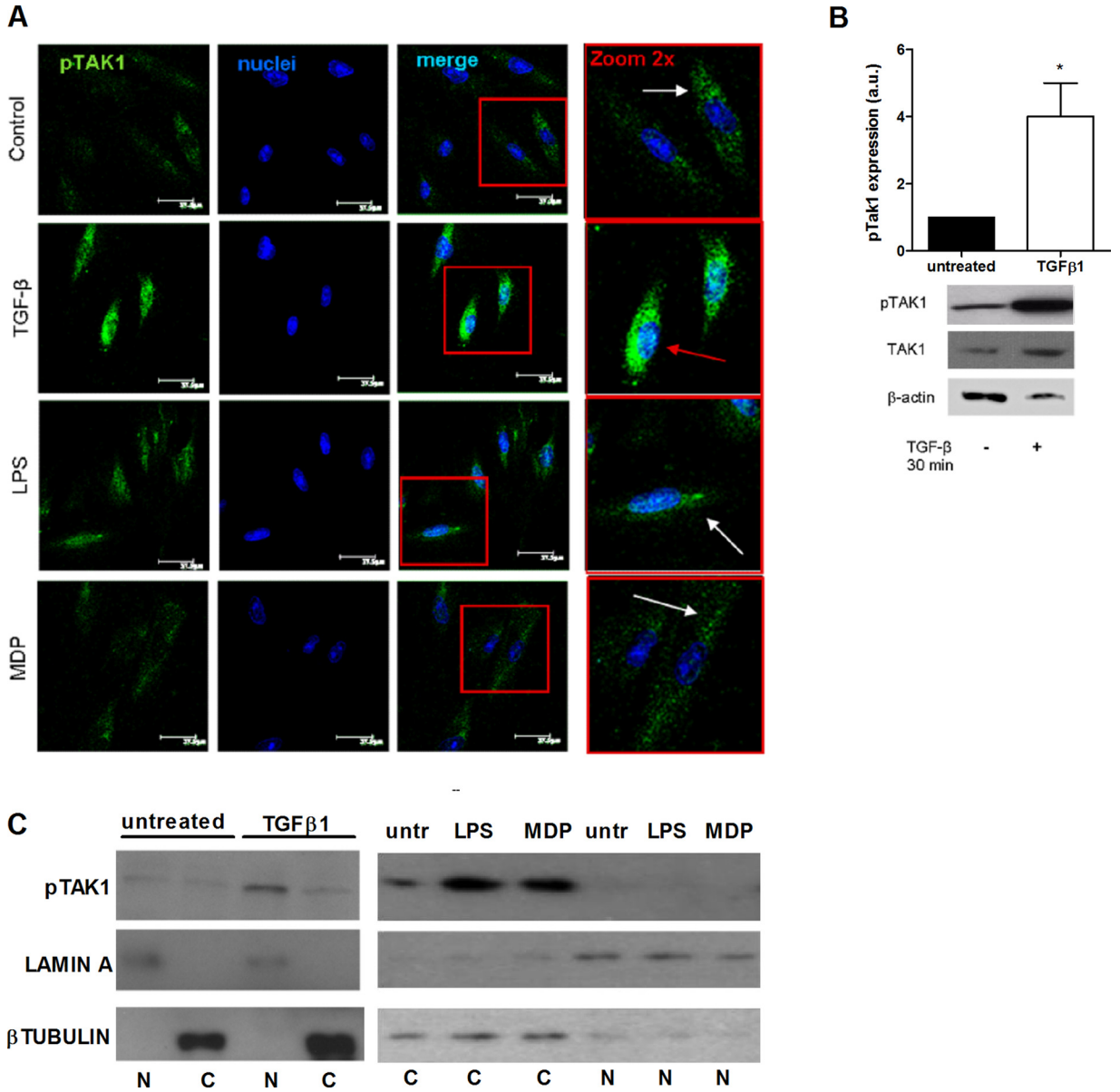

Fig. 5. pTAK1 nuclear localization following profibrogenic stimuli. *A*: representative images of immunofluorescence analysis of pTAK1 in control IMF after 30 min treatment with TGF-β, LPS, or muramyl dipeptide (MDP; scale bars, 37.5 μm; $n = 3$ for each condition). Red arrow, nuclear pTAK1$^+$; white arrows, cytoplasmic pTAK1$^+$ myofibroblasts. *B*: pTAK1 level in IMF derived from control subjects after treatment with 5 ng/ml recombinant human (rh)TGF-β for 30 min. *C*: Western blotting analysis of pTAK1 level in cytoplasmatic (C) and nuclear (N) protein fractions of IMF derived from control subjects after treatment with 5 ng/ml rhTGF-β, 1 μg/ml LPS, or 5 μg/ml MDP for 30 min. Data are reported as means ± SE of a total of 3 separate determinations with IMF derived from 3 different healthy controls. *$P < 0.01$ vs. untreated.

only TGF-β1, the main fibrogenic mediator in CD, stimulated COL1A1 mRNA expression in control and CD-derived IMF, as opposed to LPS and MDP (Fig. 6*C*).

TAK1 is required for IMF fibrogenic phenotype. To investigate the functional relevance of TAK1 in TGF-β1-induced fibrogenic phenotype in IMF, we determined the effect of TAK1 silencing or pharmacological inhibition on COL1A1 expression. The transduction of IMF with pAdshTAK1, but not with pAdshLacZ, efficiently reduced the TAK1 level in IMF (Fig. 7, *A* and *B*) and significantly reduced TGF-β1-stimulated COL1A1 mRNA expression (Fig. 7*C*). Moreover, the addition of 5Z-7-oxozeaenol confirmed the significant reduction of collagen expression and production following TAK1 inhibition (Fig. 7, *D* and *E*). Finally, to support further the role of TAK1 in the maintenance of the activated phenotype in ileal IMF, we evaluated the effect of prolonged TAK1 silencing in CD-derived IMF. As shown in Fig. 7*F*, following TAK1 silencing by shRNA, α-SMA expression decreased. Moreover, its polymerization resulted drastically impaired, as shown by immunofluorescence (Fig. 7*G*). Altogether, these data point out a fundamental role for TAK1 in the induction and support of the fibrogenic phenotype of IMF.

DISCUSSION

Tissue repair and regeneration are valuable host defense mechanisms that preserve organ integrity and function. However, if the tissue repair program does not terminate correctly

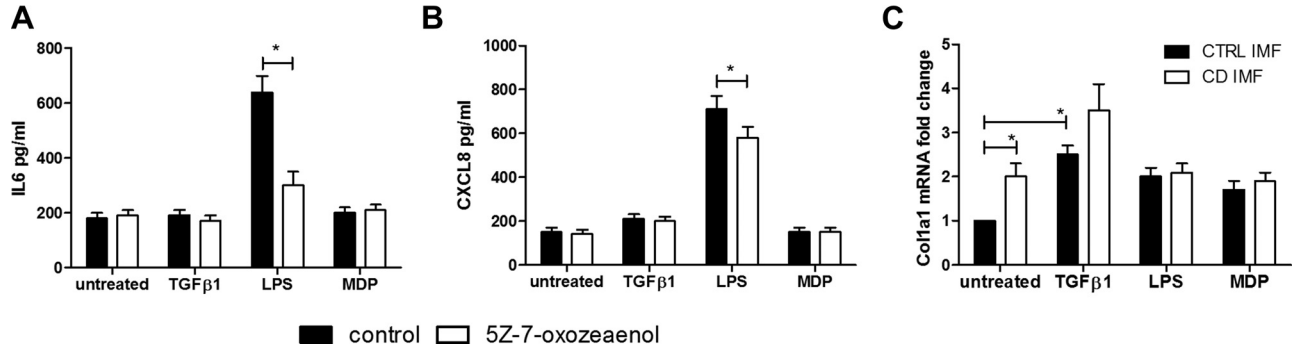

Fig. 6. TAK1 activation mediates the fibrogenic phenotype of IMF. IMFs, isolated from ileal tissues of control subjects ($n = 3$) and CD patients ($n = 3$), were treated with TGF-β1, LPS, or MDP in the presence or absence of TAK1 inhibitor 5Z-7-oxozeaenol for 12 h in the case of mRNA analysis or 24 h for cytokine quantifications ($n = 3$). IL-6 (*A*) and CXCL8 (*B*) levels were assessed by ELISA in culture supernatants. Data are reported as means ± SE. *$P < 0.01$ vs. untreated. *C*: COL1A1 mRNA expression was measured by real-time qPCR. Data are reported as means ± SE. *$P < 0.01$ vs. untreated control IMF.

because of continuous and/or recurrent tissue injury, such as in IBD, then activated myofibroblasts persist in the lesion, resulting in extensive, exaggerated synthesis of excessively contracted ECM (42). Fibrosis in CD might have devastating clinical consequences, such as development of intestinal strictures and fistulae, causing major patient morbidity (7). Although IMFs have been identified as a major player in gut fibrosis in CD, the signaling pathways generating and maintaining their fibrogenic phenotype are scarcely known. Since IMFs are strategically located in the intestinal mucosa and potentially exposed to both endogenous mediators and lumen-derived material, we focused on a peculiar MAP3K, namely TAK1, which acts at the crossroad of a variety of extracellular signals in a cell-specific manner (2, 36). We report here that the enhanced TAK1 expression and activation in the ileal mucosa of CD patients are required to maintain the fibrogenic phenotype of IMF. Furthermore, we show for the first time in primary human cells that profibrogenic but not inflammatory signals induce nuclear translocation of pTAK1.

The involvement of IMF in physiological and pathophysiological conditions of the intestine is becoming evident. In physiological conditions, IMFs contribute to ECM maintenance, stem cell niche preservation, and immune responses (39). Following chronic mucosal injuries, such as in CD patients, IMFs expand abnormally, contributing to the massive COL1A1 deposition and to gut stenosis (4). In agreement with previous reports, the IMF network in the mucosa of our CD patients directly correlated with the extent of fibrosis (39). In addition, IMF isolated from CD patients consistently maintained a fibrogenic phenotype in vitro that probably derives from the long-term in vivo exposure to mediators able to establish persistent phenotypic modifications (e.g., epigenetic signatures) (9, 11, 28, 31, 32).

The strategic position and considerable plasticity of IMF allow these cells potentially to integrate mucosal and luminal signals. To this goal, IMFs not only express receptors to endogenous cytokines, chemokines, and growth factors but also to PAMP (37). Thus in CD patients, IMF might be exposed to an excess of gut–lumen-derived PAMP, as a consequence of the enhanced mucosal permeability, and to locally produced cytokines and profibrogenic factors, such as TGF-β1. Intriguingly, the intracellular signaling pathways activated by PAMP and profibrogenic mediators, such as TGF-β1, seem to converge on TAK1, which thus might act as an integrator of these signals. However, the mechanisms by which specificity is achieved, as different stimuli lead to distinct responses in the cell, are not well characterized and require further investigation. Interestingly, TAK1 is unique among the MAP3K family members in that its activation requires complexing with a specific binding partner known as TAK1-binding protein-1, -2, -3, and -4 (TAB1, -2, -3, and -4, respectively), and the requirement of these TABs appears to be dependent on the stimuli (20, 24, 40). Furthermore, numerous studies have suggested that site-specific ubiquitination and phosphorylation on TAK1 regulate TAK1 kinase activation (2). Polyubiquitin is thought to act as a scaffold to assemble different kinase complexes, potentially conferring specificity for upstream activators, as well as downstream substrates (1). Moreover, numerous phosphorylation sites of TAK1 outside of the activation loop have also been recorded in the PhosphoSitePlus website (http://www.phosphosite.org/homeAction.do;jsessionid=9FA15C6617986B381C97C3CB0AC5B11D) and in literature (38). These post-translational modifications may finely tune TAK1 activation and subsequent, different downstream signaling events.

In agreement with previous studies conducted on the heart, kidney, and skin (16, 25, 30, 58), we report an excessive TAK1 activity during tissue remodeling associated with inflammatory insults in the gut. Altogether, these data suggest that coexistence of inflammatory stimuli and signals promoting tissue repair may cause exaggerated TAK1 activity in cells responsible for ECM deposition, eventually leading to fibrosis.

Engagement of Toll-like receptors (TLRs) on gut and liver myofibroblasts is known to elicit inflammatory programs and to enhance antigen-presenting cell functions (37, 47). However, portal endotoxemia and TLR engagement on hepatic stellate cell-derived myofibroblasts have been linked to liver fibrosis (37). Since several gene polymorphisms associated with IBD influence host responses to bacteria (54), and injection in rodents of bacteria-derived products within the gut wall leads to intestinal fibrosis (52), it was conceivable that the IMF fibrogenic phenotype could be induced directly by PAMP exposure. However, the modest effect of TLR4 and nucleotide-binding oligomerization domain 2 ligands on COL1A1 expression in control- and CD-derived IMF seems to exclude a direct profibrogenic effect of these PAMPs, although these bacterial fragments stimulate pTAK1 and cytokine release. The lack of strong fibrogenic responses to endotoxins in IMF is not sur-

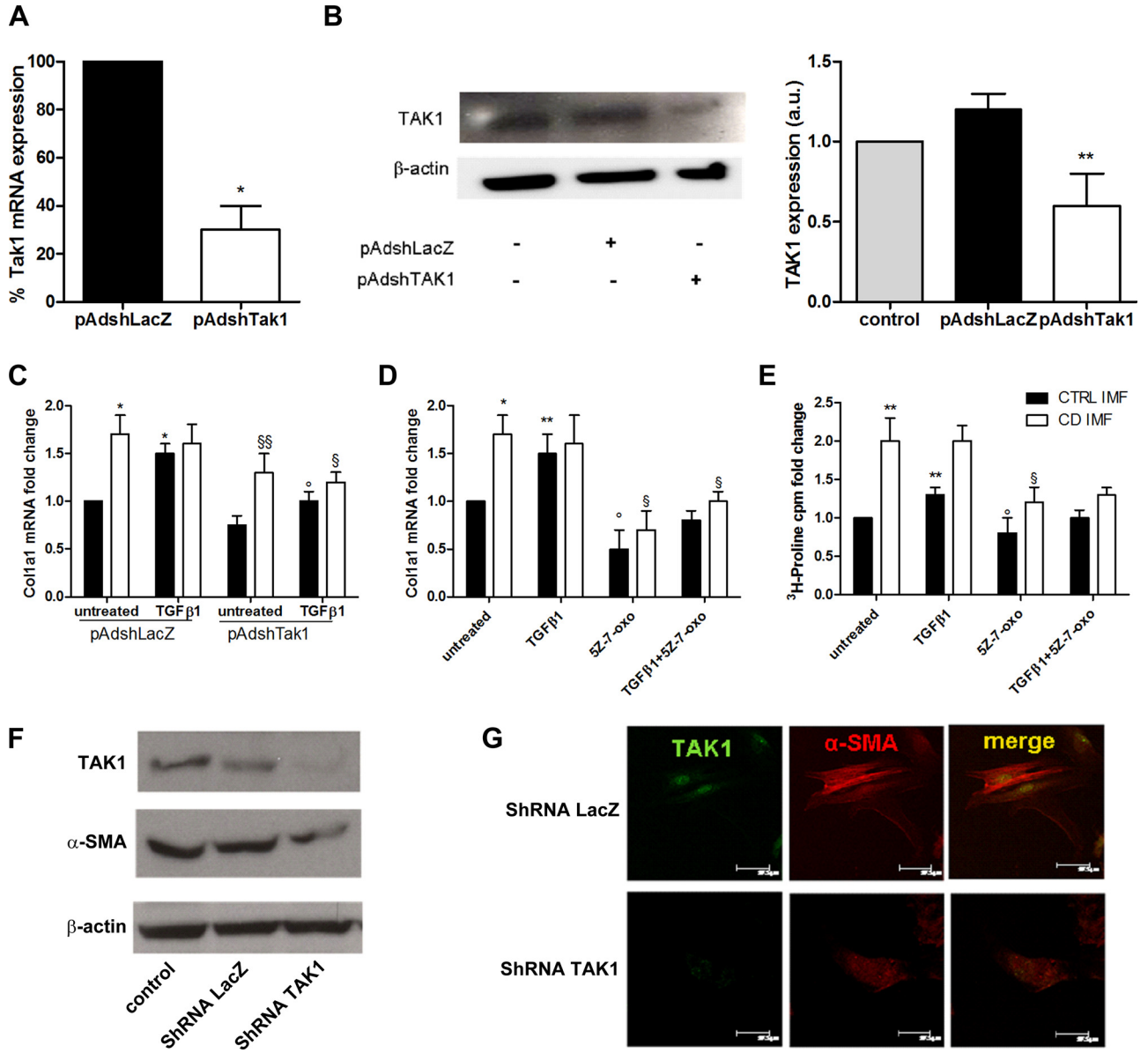

Fig. 7. TAK1 is essential for the profibrogenic phenotype of IMF. *A*: percentage of TAK1 mRNA expression after 72 h transduction with an adenoviral vector expressing shRNA targeting TAK1 (pAdshTAK1) or the gene encoding β-galactosidase (pAdshLacZ) as control ($n = 3$). *B*: Western blotting of TAK1 after 72 h transduction with pAdshTAK1 or pAdshLacZ and relative densitometric analysis. Data are reported as means ± SE of triplicate determinations of experiments performed with IMF, derived from 3 different CD patients. $*P < 0.05$ and $**P < 0.01$ vs. pAdshTAK1. *C*: real-time qPCR for COL1A1 mRNA in control- and CD-derived IMF transduced with pAdshLacZ or pAdshTAK1 for 72 h and stimulated or not with TGF-β1 for 12 h ($n = 3$ for each group). Data are reported as means ± SE. $*P < 0.01$ vs. untreated pAdshLacZ control IMF; §$P < 0.05$ and §§$P < 0.01$ vs. untreated pAdshLacZ CD IMF; °$P < 0.05$ vs. TGF-β1 pAdshLacZ control IMF. *D*: real-time qPCR for COL1A1 mRNA in control- and CD-derived IMF ($n = 3$ for each group) after 36 h treatment with 5Z-7-oxozeaenol. *E*: [^{3}H]proline incorporation in control- and CD-derived IMF ($n = 3$ for each group) and culture medium after 36 h of treatment with 5Z-7-oxozeaenol. Data are reported as means ± SE. $*P < 0.05$ and $**P < 0.01$ vs. untreated ctrl IMF; §$P < 0.05$ vs. untreated CD IMF; °$P < 0.05$ vs. TGF-β1 control IMF. *F*: Western blotting of α-SMA expression in CD-derived IMF after 6 days of transduction with pAdshTAK1 or pAdshLacZ as control ($n = 3$). *G*: representative images of immunofluorescence analysis of TAK1 and α-SMA expression in CD IMF after 6 days transduction with pAdshTAK1 or pAdshLacZ as control ($n = 3$; scale bars, 37.5 μm).

prising, since other intestinal cells, such as mucosal macrophages, are barely responsive to TLR ligands to avoid excessive release of inflammatory mediators in response to leaking bacterial products (55).

Experimental studies in mice, the analysis of gene expression in surgical specimens, and the strong fibrogenic response to TGF-β1 in IMF clearly point to the TGF-β system as the master signaling pathway in the development and maintenance of fibrosis in CD patients (6, 33, 41, 46). SMAD phosphorylation and nuclear translocation have been identified as the main intracellular TGF-β1 signaling transmission pathway also in fibrosis (6). However, experimental evidence demonstrates that other signaling molecules, such as phosphoinositide 3-kinase, Akt, mammalian target of rapamycin, Rho kinase, TNF receptor-associated factor 6, Rac, Erk, as well as TAK1, are involved in mediating TGF-β1 effects (34). In agreement with

previous studies (16, 25, 30, 58), TAK1 silencing or pharmacological inhibition with the highly selective inhibitor 5Z-7-oxozeaenol in IMF derived from normal ileal mucosa abrogated TGF-β1-induced COL1A1 gene expression and protein synthesis, supporting the relevance of TAK1 in transducing TGF-β1 fibrogenic signaling in IMF. The relevance of this observation to IBD is supported by the normalized COL1A1 gene expression and protein synthesis following TAK1 silencing or inhibition in CD-derived IMF. Furthermore, we observed that TAK1 inhibition partially depolarized α-SMA filaments in line with previous reports showing that TAK1 is critical in myofibroblast differentiation, since it stimulates the expression of cytoskeletal proteins regulating cell contraction and migration (48).

In IMF, pTAK1 was detected following exposure to proinflammatory or fibrogenic mediators. However, a fibrogenic stimulus, such TGF-β1, induced pTAK1 translocation to the nucleus, as opposed to the inflammatory stimuli, acting through TLR4–myeloid differentiating factor 88 signaling that retained pTAK1 in the cytoplasm, suggesting the existence of different regulatory mechanisms for this kinase. Recent studies have reported TAK1 translocation in the nucleus, although this kinase does not include nuclear localization sequences or the ability to regulate gene transcription directly (12, 14, 17, 22). Intriguingly, nuclear TAK1 can induce degradation of Ski-related novel protein N (SnoN), an inhibitor of SMAD transcriptional activity, boosting TGF-β1 signaling (22). Therefore, the augmented activation of TAK1 in epithelial cells regulates cytoprotective factors and cell proliferation (23, 25) and may favor epithelial-mesenchymal transition, which contributes to intestinal fibrosis (13, 14), whereas in ileal myofibroblasts, the extensive inhibition of SnoN may lead to an exaggerated SMAD transcriptional activity that includes expression of fibrosis-associated genes, although further investigation is required to substantiate this hypothesis. Differential subcellular localization of activated kinases has been reported in several systems as a factor affecting the cellular responses. Thus the same kinase activated in response to different stimuli triggers specific downstream signaling pathways, depending on the subcellular localization, providing versatility in regulating physiological responses (15, 53).

In conclusion, we report here that TAK1 expression and function are deregulated in stenotic ileal segments of CD patients and that this kinase is essential for IMF to develop and maintain a profibrogenic phenotype. Our results provide new insights into the relevance of the TAK1 signaling pathway in contributing to tissue fibrosis in CD. In taking into account the vital role of TAK1 during embryogenesis and in preserving epithelial integrity that limits the direct use of inhibitors against this kinase, modulators of downstream TAK1 effectors may represent new, alternative antifibrotic therapeutic targets (44).

ACKNOWLEDGMENTS

The authors thank Drs. Anna Rambaldo and Gloria Sarasin for technical assistance in histological sample preparation and analysis.

GRANTS

Support for this work was provided by grants from the Italian Ministry of Education, Universities and Research (PRIN 2012MZTRM3 to I. Castagliuolo and PRIN K34C45_009 to G. C. Sturniolo) and from the University of Padova (to D. Martines). A. R. Grillo was a recipient of European Crohn's and Colitis Organisation (ECCO) and Associazione Roberto Farini fellowships.

DISCLOSURES

No conflicts of interest, financial or otherwise, are declared by the authors.

AUTHOR CONTRIBUTIONS

Author contributions: A.R.G., D.M., and I.C. conception and design of research; A.R.G., Melania Scarpa, and A.B. performed experiments; A.R.G., Marco Scarpa, A.P., and R.D.C. analyzed data; A.R.G., Melania Scarpa, R.D., P.B., and D.M. interpreted results of experiments; A.R.G. and Melania Scarpa prepared figures; A.R.G. and I.C. drafted manuscript; Melania Scarpa, I.A., G.P., G.C.S., and I.C. edited and revised manuscript; A.R.G., Melania Scarpa, R.D., P.B., Marco Scarpa, A.P., R.D.C., D.M., A.B., I.A., G.P., G.C.S., and I.C. approved final version of manuscript.

REFERENCES

1. **Adhikari A, Xu M, Chen ZJ.** Ubiquitin-mediated activation of TAK1 and IKK. *Oncogene* 26: 3214–3226, 2007.
2. **Ajibade AA, Wang HY, Wang RF.** Cell type-specific function of TAK1 in innate immune signaling. *Trends Immunol* 34: 307–316, 2013.
3. **Andoh A, Bamba S, Brittan M, Fujiyama Y, Wright NA.** Role of intestinal subepithelial myofibroblasts in inflammation and regenerative response in the gut. *Pharmacol Ther* 114: 94–106, 2007.
4. **Andoh A, Fujino S, Okuno T, Fujiyama Y, Bamba T.** Intestinal subepithelial myofibroblasts in inflammatory bowel diseases. *J Gastroenterol* 37: 33–37, 2007.
5. **Atfi A, Djelloul S, Chastre E, Davis R, Gespach C.** Evidence for a role of Rho-like GTPases and stress-activated protein kinase/c-Jun N-terminal (SAPK/JNK) in transforming growth factor beta-mediated signaling. *J Biol Chem* 272: 1429–1432, 1997.
6. **Biernacka A, Dobaczewski M, Frangogiannis NG.** TGF-β signaling in fibrosis. *Growth Factors* 29: 196–202, 2011.
7. **Burke JP, Mulsow JJ, O'Keane C, Docherty NG, Watson RW, O'Connell PR.** Fibrogenesis in Crohn's disease. *Am J Gastroenterol* 102: 439–448, 2007.
8. **Cosnes J, Cattan S, Blain A, Beaugerie L, Carbonnel F, Parc R, Gendre JP.** Long-term evolution of disease behavior of Crohn's disease. *Inflamm Bowel Dis* 8: 244–250, 2002.
9. **Cunningham MF, Docherty NG, Burke JP, O'Connell PR.** S100A4 expression is increased in stricture fibroblasts from patients with fibrostenosing Crohn's disease and promotes intestinal fibroblast migration. *Am J Physiol Gastrointest Liver Physiol* 299: G457–G466, 2010.
10. **Derynck R, Zhang YE.** Smad-dependent and Smad-independent pathways in TGF-beta family signalling. *Nature* 425: 577–584, 2003.
11. **Di Sabatino A, Pender SL, Jackson CL, Prothero JD, Gordon JN, Picariello L, Rovedatti L, Docena G, Monteleone G, Rampton DS, Tonelli F, Corazza GR, MacDonald TT.** Functional modulation of Crohn's disease myofibroblasts by anti-tumor necrosis factor antibodies. *Gastroenterology* 133: 137–149, 2007.
12. **Ear T, Fortin CF, Simard FA, McDonald PP.** Constitutive association of TGF-beta-activated kinase 1 with the IkappaB kinase complex in the nucleus and cytoplasm of human neutrophils and its impact on downstream processes. *J Immunol* 184: 3897–3906, 2010.
13. **Flier SN, Tanjore H, Kokkotou EG, Sugimoto H, Zeisberg M, Kalluri R.** Identification of epithelial to mesenchymal transition as a novel source of fibroblasts in intestinal fibrosis. *J Biol Chem* 285: 20202–20212, 2010.
14. **Gardner A, Fisher AJ, Richter C, Johnson GE, Moisey EJ, Brodlie M, Ward C, Krippner-Heidenreich A, Mann DA, Borthwick LA.** The critical role of TAK1 in accentuated epithelial to mesenchymal transition in obliterative bronchiolitis after lung transplantation. *Am J Pathol* 180: 2293–2308, 2012.
15. **Gomel R, Xiang C, Finniss S, Lee HK, Lu W, Okhrimenko H, Brodie C.** The localization of protein kinase C δ in different subcellular sites affects its proapoptotic and antiapoptotic functions and the activation of distinct downstream signaling pathways. *Mol Cancer Res* 5: 627–639, 2007.
16. **Guo F, Hutchenreuther J, Carter DE, Leask A.** TAK1 is required for dermal wound healing and homeostasis. *J Invest Dermatol* 133: 1646–1654, 2013.
17. **Hanafusa H, Ninomiya-Tsuji J, Masuyama N, Nishita M, Fujisawa J, Shibuya H, Matsumoto K, Nishida E.** Involvement of the p38 mitogen-activated protein kinase pathway in transforming growth factor-beta-induced gene expression. *J Biol Chem* 274: 27161–27167, 1999.
18. **Hinz B, Phan SH, Thannickal VJ, Prunotto M, Desmoulière A, Varga J, De Wever O, Mareel M, Gabbiani G.** Recent developments in

myofibroblast biology: paradigms for connective tissue remodeling. *Am J Pathol* 180: 1340–1355, 2012.
19. **Hocevar BA, Prunier C, Howe PH.** Disabled-2 (Dab2) mediates transforming growth factor beta (TGFbeta)-stimulated fibronectin synthesis through TGFbeta-activated kinase 1 and activation of the JNK pathway. *J Biol Chem* 280: 25920–25927, 2005.
20. **Inagaki M, Omori E, Kim JY, Komatsu Y, Scott G, Ray MK, Yamada G, Matsumoto K, Mishina Y, Ninomiya-Tsuji J.** TAK1-binding protein 1, TAB1, mediates osmotic stress-induced TAK1 activation but is dispensable for TAK1-mediated cytokine signaling. *J Biol Chem* 283: 33080–33086, 2008.
21. **Irie T, Muta T, Takeshige K.** TAK1 mediates an activation signal from Toll-like receptor(s) to nuclear factor-κB in lipopolysaccharide-stimulated macrophages. *FEBS Lett* 467: 160–164, 2000.
22. **Kajino T, Omori E, Ishii S, Matsumoto K, Ninomiya-Tsuji J.** TAK1 MAPK kinase kinase mediates transforming growth factor-beta signaling by targeting SnoN oncoprotein for degradation. *J Biol Chem* 282: 9475–9481, 2007.
23. **Kajino-Sakamoto R, Omori E, Nighot PK, Blikslager AT, Matsumoto K, Ninomiya-Tsuji J.** TGF-beta-activated kinase 1 signaling maintains intestinal integrity by preventing accumulation of reactive oxygen species in the intestinal epithelium. *J Immunol* 185: 4729–4737, 2010.
24. **Kanayama A, Seth RB, Sun L, Ea CK, Hong M, Shaito A, Chiu YH, Deng L, Chen ZJ.** TAB2 and TAB3 activate the NF-κB pathway through binding to polyubiquitin chains. *Mol Cell* 15: 535–548, 2004.
25. **Kim JY, Kajino-Sakamoto R, Omori E, Jobin C, Ninomiya-Tsuji J.** Intestinal epithelial-derived TAK1 signaling is essential for cytoprotection against chemical-induced colitis. *PLoS One* 4: e4561, 2009.
26. **Kim SI, Kwak JH, Zachariah M, He Y, Wang L, Choi ME.** TGF-beta-activated kinase 1 and TAK1-binding protein 1 cooperate to mediate TGF-beta1-induced MKK3-p38 MAPK activation and stimulation of type I collagen. *Am J Physiol Renal Physiol* 292: F1471–F1478, 2007.
27. **Kishimoto K, Matsumoto K, Ninomiya-Tsuji J.** TAK1 mitogen-activated protein kinase kinase kinase is activated by autophosphorylation within its activation loop. *J Biol Chem* 275: 7359–7364, 2000.
28. **Lang M, Schlechtweg M, Kellermeier S, Brenmoehl J, Falk W, Schölmerich J, Herfarth H, Rogler G, Hausmann M.** Gene expression profiles of mucosal fibroblasts from strictured and nonstrictured areas of patients with Crohn's disease. *Inflamm Bowel Dis* 15: 212–223, 2009.
29. **Mahida YR, Beltinger J, Makh S, Göke M, Gray T, Podolsky DK, Hawkey CJ.** Adult human colonic subepithelial myofibroblasts express extracellular matrix proteins and cyclooxygenase-1 and -2. *Am J Physiol Gastrointest Liver Physiol* 273: G1341–G1348, 1997.
30. **Matsumoto-Ida M, Takimoto Y, Aoyama T, Akao M, Takeda T, Kita T.** Activation of TGF-beta1-TAK1-p38 MAPK pathway in spared cardiomyocytes is involved in left ventricular remodeling after myocardial infarction in rats. *Am J Physiol Heart Circ Physiol* 290: H709–H715, 2006.
31. **McKaig BC, Hughes K, Tighe PJ, Mahida YR.** Differential expression of TGF-beta isoforms by normal and inflammatory bowel disease intestinal myofibroblasts. *Am J Physiol Cell Physiol* 282: C172–C182, 2002.
32. **McKaig BC, McWilliams D, Watson SA, Mahida YR.** Expression and regulation of tissue inhibitor of metalloproteinase-1 and matrix metalloproteinases by intestinal myofibroblasts in inflammatory bowel disease. *Am J Pathol* 162: 1355–1360, 2003.
33. **Mola FF, Friess H, Scheuren A, Di Sebastiano P, Graber H, Egger B, Zimmermann A, Korc M, Büchler MW.** Transforming growth factor-betas and their signaling receptors are coexpressed in Crohn's disease. *Ann Surg* 229: 67–75, 1999.
34. **Mu Y, Gudey SK, Landström M.** Non-Smad signaling pathways. *Cell Tissue Res* 347: 11–20, 2011.
35. **Ninomiya-Tsuji J, Kishimoto K, Hiyama A, Inoue J, Cao Z, Matsumoto K.** The kinase TAK1 can activate the NIK-I kappaB as well as the MAP kinase cascade in the IL-1 signalling pathway. *Nature* 398: 252–256, 1999.
36. **Ono K, Ohtomo T, Ninomiya-Tsuji J, Tsuchiya M.** A dominant negative TAK1 inhibits cellular fibrotic responses induced by TGF-beta. *Biochem Biophys Res Commun* 307: 332–337, 2003.
37. **Otte JM, Rosenberg IM, Podolsky DK.** Intestinal myofibroblasts in innate immune responses of the intestine. *Gastroenterology* 124: 1866–1878, 2003.
38. **Ouyang C, Nie L, Gu M, Wu A, Han X, Wang X, Shao J, Xia Z.** Transforming growth factor (TGF)-β-activated kinase 1 (TAK1) activation requires phosphorylation of serine 412 by protein kinase A catalytic subunit α (PKACα) and X-linked protein kinase (PRKX). *J Biol Chem* 289: 24226–24237, 2014.
39. **Powell DW, Pinchuk IV, Saada JI, Chen X, Mifflin RC.** Mesenchymal cells of the intestinal lamina propria. *Annu Rev Physiol* 73: 213–237, 2011.
40. **Prickett TD, Ninomiya-Tsuji J, Broglie P, Muratore-Schroeder TL, Shabanowitz J, Hunt DF, Brautigan DL.** TAB4 stimulates TAK1-TAB1 phosphorylation and binds polyubiquitin to direct signaling to NF-kappaB. *J Biol Chem* 283: 19245–19254, 2008.
41. **Pucilowska JB, Williams KL, Lund PK.** Fibrogenesis IV. Fibrosis and inflammatory bowel disease: cellular mediators and animal models. *Am J Physiol Gastrointest Liver Physiol* 279: G653–G659, 2000.
42. **Rieder F, Brenmoehl J, Leeb S, Schölmerich J, Rogler G.** Wound healing and fibrosis in intestinal disease. *Gut* 56: 130–139, 2007.
43. **Rutgeerts P, Geboes K, Vantrappen G, Beyls J, Kerremans R, Hiele M.** Predictability of the postoperative course of Crohn's disease. *Gastroenterology* 99: 956–963, 1990.
44. **Sakurai H.** Targeting of TAK1 in inflammatory disorders and cancer. *Trends Pharmacol Sci* 33: 522–530, 2012.
45. **Sakurai H, Suzuki S, Kawasaki N, Nakano H, Okazaki T, Chino A, Doi T, Saiki I.** Tumor necrosis factor-alpha-induced IKK phosphorylation of NF-kappaB p65 on serine 536 is mediated through the TRAF2, TRAF5, and TAK1 signaling pathway. *J Biol Chem* 278: 36916–36923, 2003.
46. **Scarpa M, Bortolami M, Morgan SL, Kotsafti A, Ruffolo C, D'Incà R, Bertin E, Polese L, D'Amico DF, Sturniolo GC, Angriman I.** TGF-beta1 and IGF-1 and anastomotic recurrence of Crohn's disease after ileo-colonic resection. *J Gastrointest Surg* 12: 1981–1990, 2008.
47. **Schwabe RF, Seki E, Brenner DA.** Toll-like receptor signaling in the liver. *Gastroenterology* 130: 1886–1900, 2006.
48. **Shi-wen X, Parapuram SK, Pala D, He Y, Wang L, Choi ME.** Requirement of transforming growth factor beta-activated kinase 1 for transforming growth factor beta-induced alpha-smooth muscle actin expression and extracellular matrix contraction in fibroblasts. *Arthritis Rheum* 60: 234–241, 2009.
49. **Shirakabe K, Yamaguchi K, Shibuya H, Irie K, Matsuda S, Moriguchi T, Gotoh Y, Matsumoto K, Nishida E.** TAK1 mediates the ceramide signaling to stress-activated protein kinase/c-Jun N-terminal kinase. *J Biol Chem* 272: 8141–8144, 1997.
50. **Singhirunnusorn P, Suzuki S, Kawasaki N, Saiki I, Sakurai H.** Critical roles of threonine 187 phosphorylation in cellular stress-induced rapid and transient activation of transforming growth factor-beta-activated kinase 1 (TAK1) in a signaling complex containing TAK1-binding protein TAB1 and TAB2. *J Biol Chem* 280: 7359–7368, 2005.
51. **Ulmasov B, Xu Z, Tetri LH, Inagami T, Neuschwander-Tetri BA.** Protective role of angiotensin II type 2 receptor signaling in a mouse model of pancreatic fibrosis. *Am J Physiol Gastrointest Liver Physiol* 296: G284–G294, 2009.
52. **Van-Tol EA, Holt L, Li FL, Kong FM, Rippe R, Yamauchi M, Pucilowska J, Lund PK, Sartor RB.** Bacterial cell wall polymers promote intestinal fibrosis by direct stimulation of myofibroblasts. *Am J Physiol Gastrointest Liver Physiol* 277: G245–G255, 1999.
53. **Vincent O, Townley R, Kuchin S, Carlson M.** Subcellular localization of the Snf1 kinase is regulated by specific beta subunits and a novel glucose signaling mechanism. *Genes Dev* 15: 1104–1114, 2001.
54. **Waterman M, Xu W, Stempak JM, Milgrom R, Bernstein CN, Griffiths AM, Greenberg GR, Steinhart AH, Silverberg MS.** Distinct and overlapping genetic loci in Crohn's disease and ulcerative colitis: correlations with pathogenesis. *Inflamm Bowel Dis* 17: 1936–1942, 2011.
55. **Wimmer N, Huber B, Barabas N, Röhrl J, Pfeffer K, Hehlgans T.** Lymphotoxin β receptor activation on macrophages induces cross-tolerance to TLR4 and TLR9 ligands. *J Immunol* 188: 3426–3433, 2012.
56. **Wynn TA.** Cellular and molecular mechanisms of fibrosis. *J Pathol* 214: 199–210, 2008.
57. **Yamaguchi K, Shirakabe K, Shibuya H, Irie K, Oishi I, Ueno N, Taniguchi T, Nishida E, Matsumoto K.** Identification of a member of the MAPKKK family as a potential mediator of TGF-beta signal transduction. *Science* 270: 2008–2011, 1995.
58. **Zhang D, Gaussin V, Taffet GE, Belaguli NS, Yamada M, Schwartz RJ, Michael LH, Overbeek PA, Schneider MD.** TAK1 is activated in the myocardium after pressure overload and is sufficient to provoke heart failure in transgenic mice. *Nat Med* 6: 556–563, 2000.